ELSEVIER

Nuclear Engineering and Design 150 (1994) 61-68

Nuclear Engineering and Design

Calculating decay heat removal rates via natural circulation along variable heat flux reactor fuel plates

M.A. Langerman

South Dakota School of Mines and Technology, Rapid City, SD 57701-3995, USA

Abstract

A recently developed integral technique is applied to natural convection cooling along test reactor fuel plates. The technique is demonstrated for water and air flow. In the case of air flow, the process is characterized by a large temperature rise along the fuel channel, thereby rendering the commonly applied Boussinesq approximation invalid. This case is a heat transfer problem of particular interest in accident analyses such as determining the level of decay heat dissipation possible, without exceeding the melting temperature of the fuel, subsequent to a hypothetical loss of primary coolant.

1. Introduction

Many reactors that are designed to generate high neutron fluxes use metallic, plate-type nuclear fuel. These reactors contain compact cores made up of fuel elements consisting of several closely spaced, thin, parallel fuel plates forming large aspect ratio flow channels. These fuel plates are usually arranged in either a flat or an annular channel geometry within the fuel elements.

After irradiation, the fuel assemblies are removed to storage ponds, water-filled canals, or some similar facility designed to provide a safe environment for handling radioactive materials. For design and accident analyses, it is necessary to estimate the fuel decay heat removal rate by means of natural circulation of water or, in the unlikely event of an accident and prolonged atmospheric exposure, natural circulation of air. In either case, the objective is to determine the maximum fuel plate (critical) power that can be dissipated via natural circulation without exceeding the ambient saturation temperature, in the case of water flow, or the melting temperature of the fuel, in the case of air flow. Since large temperature rises may result, fluid property variations may become significant.

1.1. Background

Over the last 20 years, research in natural convection has concentrated on problems involving a low temperature ratio T_R, where T_R is defined as the ratio of the channel outlet mean fluid temperature to the channel average fluid temperature (Langerman, 1993). With a low T_R, the problem is amenable to the simplifying Boussinesq approximation, which is commonly under-

SSDI 0029-5493(94)00642-C

stood (Gray, 1976) to consist of the assumptions that (a) the fluid properties are constant except density in the momentum equation when it directly causes buoyant forces and (b) viscous dissipation is negligible. Langerman and Bayless (1992), however, showed in their analysis of nuclear fuel that the effect of property variations along the channel is important and must be taken into account. In a recent development (Langerman, 1993) an integral method is described for calculating natural circulation, for processes involving a large T_R, along channels subjected to uniform heat fluxes. This technique is expanded in this paper to the variable heat flux boundary condition necessary for calculating the critical fuel plate power.

2. Statement of problem

It is assumed in this analysis that the flow is laminar boundary layer flow and that the velocity and temperature fields are adequately represented as two-dimensional, fully developed fields between vertical parallel plates that are heated symmetrically. The laminar flow assumption is justified on the basis of results from Miyamoto et al. (1982) who show that laminar flow is predominant for $\mathrm{Pr}\,\mathrm{Gr}_L \leq 10^{11-12}$, where Gr_L is calculated using the overall plate length. Over the range of heat fluxes relevant to this analysis, $\mathrm{Pr}\,\mathrm{Gr}_L$ is on the order of 10^{10}.

Boundary layer flow is a good assumption for channel aspect ratios R greater than 15 (Ramanathan, 1991). Channel aspect ratios in test reactors are commonly 500 or greater, and therefore the effects of axial diffusion should be negligible and the treatment as boundary layer flow an appropriate simplification.

Assuming fully developed velocity and temperature profiles, and thereby neglecting the effect of the hydrodynamic and thermal entry lengths, is a non-conservative assumption with regard to critical power level estimates but probably of negligible consequence here because of the relatively short entry lengths associated with large channel aspect ratios (Ramanathan, 1991).

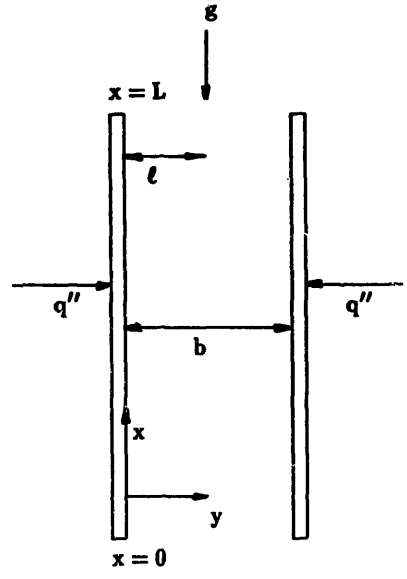

Fig. 1. Flow model.

2.1. Integral analysis

The integral boundary layer equations are written below in Cartesian coordinates. As shown in Fig. 1, the x direction is the direction of flow along the channel and the y direction is the direction normal to the plate. The equations for mass, momentum, and energy are respectively

$$\frac{\mathrm{d}}{\mathrm{d}x}\int_0^l \rho u \,\mathrm{d}y = 0 \tag{1}$$

$$-\frac{\mathrm{d}}{\mathrm{d}x}\int_0^l \rho u^2 \,\mathrm{d}y - \tau_0 - \int_0^l \rho g \,\mathrm{d}y - \frac{\mathrm{d}p}{\mathrm{d}x} l = 0 \tag{2}$$

and

$$\frac{\mathrm{d}}{\mathrm{d}x}\int_0^l \rho c_p u(T - T_\infty)\,\mathrm{d}y - q'' = 0 \tag{3}$$

where l is the distance from the plate to the channel line of symmetry (i.e. half the channel gap width), ρ is the fluid density, u is the local fluid velocity, T and T_∞ are the local and channel inlet fluid temperatures respectively, c_p is the fluid specific heat, τ_0 is the channel wall shear stress and q'' is the symmetric channel wall heat flux. At this point, the governing equations are unconstrained, in a boundary layer sense, except for the assumption of fully developed, low velocity flow.

The boundary conditions are

$$\text{at } y = 0, \quad \frac{\partial T}{\partial y} = -\frac{q''}{k}$$

and

$$\text{at } y = l, \quad \frac{\partial T}{\partial y} = 0 \tag{4}$$

The facility in applying the integral boundary layer approach lies in the resulting solution of ordinary differential equations as opposed to partial differential equations. This approach, however, requires representations for the velocity and temperature distributions and the wall shear stress. Indeed, the solution accuracy is dependent on these representations. Langerman and Bayless (1992) showed that, for laminar, Newtonian, Boussinesq natural circulation, simple parabolic distributions produced results indistinguishable from those of Aung (1972), who solved the problem using a partial differential equation approach. These distributions are used in this analysis and are given here in terms of the local mean channel velocity V, the local mean channel temperature T_m and the local mean fuel plate surface temperature T_0 as

$$u = \frac{3}{2} V\left(\frac{2y}{l} - \frac{y^2}{l^2}\right)$$

and

$$T = T_0 + \frac{5}{4}(T_0 - T_m)\left(\frac{y^2}{l^2} - \frac{2y}{l}\right) \tag{5}$$

As in most natural circulation analyses, the fluid density is assumed to vary as a linear function of temperature as

$$\rho = \tilde{\rho} - [1 - \tilde{\beta}(T - \tilde{T})] \tag{6}$$

where the tilde indicates an average value over some length Δx along the channel and β is the coefficient of thermal expansion defined as

$$\beta = -\frac{1}{\rho}\left(\frac{\partial \rho}{\partial T}\right)_p \tag{7}$$

Substituting Eq. (6) (with a similar relation for fluid viscosity) into Eq. (2), it can be shown (Langerman, 1993) that the velocity gradient along the channel varies as

$$\frac{dV}{dx} = -\frac{2.5\tilde{\mu}[1 + \tilde{\sigma}(T_0 - \tilde{T})]}{\tilde{\rho} l^2 [1 + 2\tilde{\beta}(\tilde{T} - T_m)]} + \frac{g\tilde{\beta}}{V[1 + 2\tilde{\beta}(\tilde{T} - T_m)]} \times \left[\frac{5}{6}(T_0 - \tilde{T}) - \frac{25}{36}(T_0 - T_m)\right] - \frac{5}{6V[1 + 2\tilde{\beta}(\tilde{T} - T_m)]}\left(\frac{1}{\tilde{\rho}}\frac{d\hat{p}}{dx} + g\right) \tag{8}$$

where $d\hat{p}/dx$ is an estimate of the local channel pressure gradient obtained from a first-order approximation of the integral momentum equation (Langerman, 1993). In Eq. (8), $\tilde{\sigma}(T_0 - \tilde{T})$ accounts for the change in viscosity around $\tilde{T}$ and essentially admits another "body force" like term to the equation of motion. Information regarding the temperature T_m is obtained by integrating Eq. (3) along Δx. The constant heat flux boundary condition data are used to relate T_0 and T_m via Fourier's law.

It is easily shown that Eq. (8), under Boussinesq fluid conditions, reduces to the well-known closed form solution first published by Aung (1972),

$$V = 0.2887\, \mathrm{Ra}^{1/2}\, \tilde{\nu} L/\mathrm{Pr}\, b^2 \tag{9}$$

Results obtained from Eq. (9) will be used as a comparison with results from the non-Boussinesq model.

For convenience, Eq. (8) is cast in non-dimensional form as

$$\frac{dV^*}{dx^*} = \frac{\tilde{\mathrm{Pr}}\, \tilde{\mathrm{Ra}}}{V^* \tilde{\omega}}\left[\frac{5}{6}\left(\frac{\Delta x^*}{V^*} - \frac{d\hat{p}^*}{dx^*}\right) + \frac{1}{36}\right] - 10\, \tilde{\mathrm{Pr}}\, \frac{\tilde{\psi}}{\tilde{\omega}} \tag{10}$$

In Eq. (10), $\tilde{\mathrm{Pr}}$ is the local average Prandtl number, $\tilde{\mathrm{Ra}}$ is the local average Rayleigh number, $\tilde{\omega} = 1 + 2(\partial\rho/\partial T)(\tilde{T} - T_m)$, and $\tilde{\psi} = 1 + (\partial u/\partial T)(T_0 - \tilde{T})$. The problem described by Eq. (10) is not particularly well suited to dimensional analysis since $\tilde{\mathrm{Ra}}$ and, to a lesser extent, $\tilde{\mathrm{Pr}}$ are local parameters that vary along the channel. The solution procedure (Langerman, 1993), therefore, begins by specifying a channel wall heat flux

and mass flow rate. The local values of $\widetilde{\mathrm{Pr}}$ and $\widetilde{\mathrm{Ra}}$ are determined and Eq. (10) is integrated, using a fourth-order Runge–Kutta scheme, along an incremental length of the channel. The estimated pressure gradient is then modified, if necessary, using

$$\left.\frac{d\hat{p}^*}{dx^*}\right|^{n+1} = \left.\frac{d\hat{p}^*}{dx^*}\right|^{n} + \Delta\left(\frac{d\hat{p}^*}{dx^*}\right) \tag{11}$$

where n is the iteration number and $\Delta(\,)$ is the correction term that drives the solution towards a numerical measure of continuity. This correction term is obtained from (Langerman, 1993):

$$\Delta\left(\frac{d\hat{p}^*}{dx^*}\right) = -\frac{2V^*(\Delta V^*)}{\Delta x^*}\frac{R}{\widetilde{\mathrm{Pr}}\,\widetilde{\mathrm{Ra}}} \tag{12}$$

where ΔV^* is the difference between the velocity obtained with the assumed mass flow rate and fluid state changes over Δx^* and the velocity obtained from Eq. (10). This procedure is continued along the entire channel length at which point the outlet pressure $\hat{p}^*$ is compared with the implied null boundary condition, $\hat{p}^* = 0$. If a significant difference results, the calculation is restarted with a newly assumed value of the mass flow rate and the loop continued until $\hat{p}^* \leq \epsilon$, where ϵ is an acceptable numerical measure of zero. The calculated fuel plate surface temperature at the channel outlet, which (with a uniform heat flux) is the location of the maximum fuel plate temperature, is then compared with the analysis objective and the steps are repeated, if necessary, with a new set of initial assumptions.

The present problem is additionally complicated by the fact that the heat flux is not uniform along the channel but typically varies in a skewed cosine profile, such as

$$q''(x) = \gamma_{\mathrm{pf}} q''_{\mathrm{avg}} \cos[a_0(a_1 x - a_2)] \tag{13}$$

where coefficients a_i are system dependent, γ_{pf} is the channel peaking factor and q''_{avg} is the average overall channel heat flux. The local average heat flux is obtained from Eq. (13) as

$$q''(\tilde{x}) = \frac{1}{\Delta x}\int_{\Delta x} \gamma_{\mathrm{pf}} q''_{\mathrm{avg}} \cos[a_0(a_1 x - a_2)]\,dx \tag{14}$$

It should be noted that, for non-analytic power distributions, the right-hand side of Eq. (14) should be evaluated using a quadrature scheme of an accuracy compatible with the integration scheme used to solve Eq. (10). Results obtained from this analysis are discussed in the following section.

Remark

The analysis here does not consider heat loss through conduction or radiation out of the ends or sides of the fuel assemblies. In practice, therefore, the critical plate power obtained will be a conservative estimate.

3. Analysis results and discussion

Results are presented here in terms of a non-dimensional heat flux Φ and a non-dimensional parameter Λ where (Langerman, 1993)

$$\Phi = \frac{q''L}{(Tk)_\infty} \tag{15}$$

and

$$\Lambda = \left[\Phi\left(\frac{R}{S}\right)^3\right]^{1/2} \tag{16}$$

and where k is the fluid thermal conductivity, L is the length of the fuel plates, and S is the ratio of L to unit depth. The subscript ∞ in Eq. (15) indicates that the parenthetical quantities are evaluated at ambient atmospheric conditions. This presentation of results is convenient since both Φ and Λ are known a priori.

3.1. Air flow

Fig. 2 shows the calculated non-dimensional mass flow rate M^* vs. Λ, where

$$M^* = \frac{\dot{m}(c_{\mathrm{p}}T)_\infty}{q''_{\mathrm{avg}}L} \tag{17}$$

In Eq. (17), $\dot{m}$ is the channel mass flow rate and c_{p} is the fluid specific heat. The results presented are for both a uniform heat flux (based on the average channel heat flux) and a non-uniform heat flux (obtained from Eq. (14)). Also included for information purposes is the Boussinesq approximation in which Eq. (8) reduces to Eq. (9).

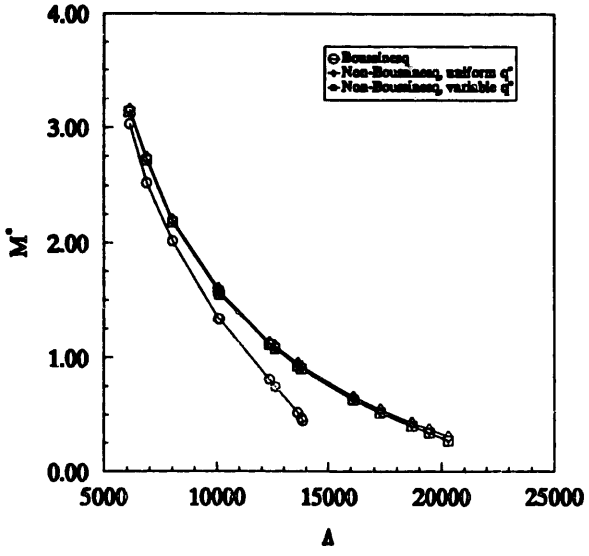

Fig. 2. Non-dimensional mass flow rate for air flow, $T_\infty = 300$ K.

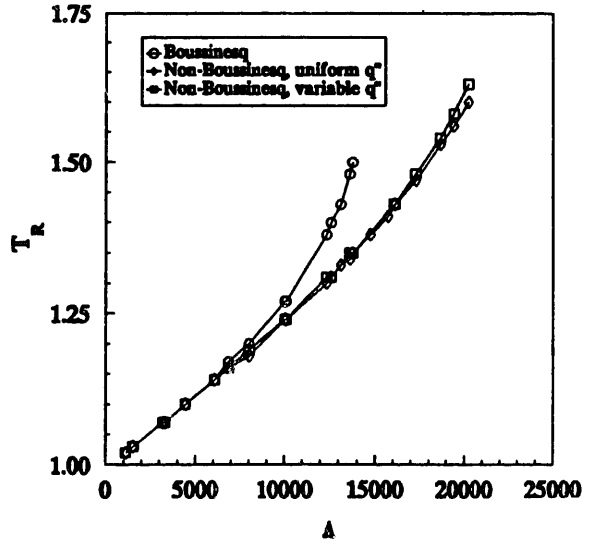

Fig. 3. Temperature ratio for air flow, $T_\infty = 300$ K.

As indicated, the channel flow rate is not particularly sensitive to the variable heat flux distribution for $\Lambda < 1.5 \times 10^4$. For $\Lambda > 1.5 \times 10^4$, the flow rate calculated with the variable heat flux is slightly less than that calculated with a uniform heat flux. The data also indicate that the flow rate obtained with the Boussinesq model is substantially lower than that obtained with the non-Boussinesq model, particularly for $\Lambda > 10^4$. This is consistent with results given in Langerman and Bayless (1992).

Fig. 3 shows T_R vs. Λ for an inlet fluid temperature of 300 K. The slightly lower flow rate obtained with the non-uniform heat flux and indicated in Fig. 2 for $\Lambda > 1.5 \times 10^4$ is reflected in the slightly higher T_R in Fig. 3. Once again, the Boussinesq results are included for comparison and indicate substantially higher values of T_R for $\Lambda > 10^4$.

If it is assumed that the fuel melting temperature is 900 K (Langerman, 1992), then $T_{R_c} = 1.5$, where the subscript c means critical. From Fig. 3 at $T_R = 1.5$, $\Lambda_c \approx 1.8 \times 10^4$. At this value of Λ, the effect of a variable heat flux is insignificant. The critical heat flux Φ_c is, therefore,

$$\Phi_c = \frac{(1.8 \times 10^4)^2}{(R/S)^3} \tag{18}$$

Fig. 4 presents a plot of Φ_c *vs.* R/S. Eq. (18) (or Fig. 4) is a very useful relationship for determining critical fuel powers since the only input needed is the channel geometry. For example, given $R = 610$ and $L = 1.22$ m, then from Eq. (18), $\Phi_c = 2.6$. From Eq. (15), with $k_\infty = 0.026$ W m^{-1} K^{-1} and $T_\infty = 300$ *K*, $q''_{avg_c} = 17$ W m^{-2}.

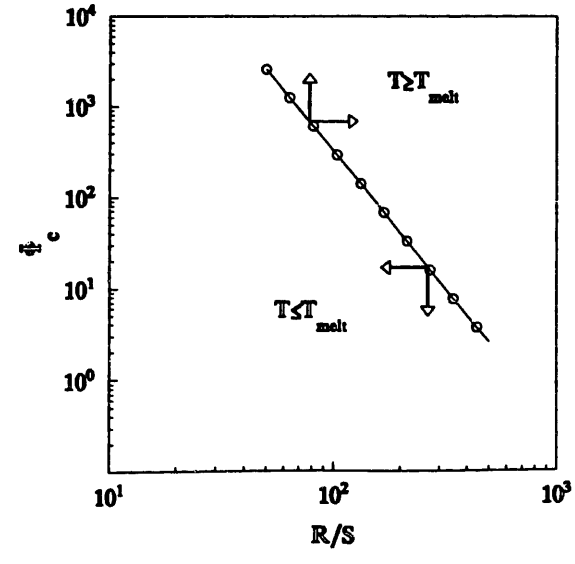

Fig. 4. Critical heat flux for air flow, $T_\infty = 300$ K.

3.2. Water flow

With water flow comes much higher flow rates along the channel and correspondingly higher channel heat fluxes. With the temperature distribution given by Eq. (5), the relation between the wall and fluid temperature difference and the heat flux is given by

$$T_0 - T_m = \frac{q''b}{5k} \tag{19}$$

Since the thermal conductivity for liquid water, at ambient pressure, is approximately constant, the temperature difference, for a specified channel geometry, is directly proportional to the heat flux. Similarly, the temperature difference, given a specified heat flux, is directly proportional to the channel gap width or, at constant channel lengths, inversely proportional to the channel aspect ratio R.

The relatively large temperature difference between the wall and the fluid resulting from a combination of high heat flux and small aspect ratio complicates the task of quantifying Φ_c. For example, Fig. 5 shows the non-dimensional wall temperature T_0^* for the case of a non-uniform heat flux. Included are the results obtained using

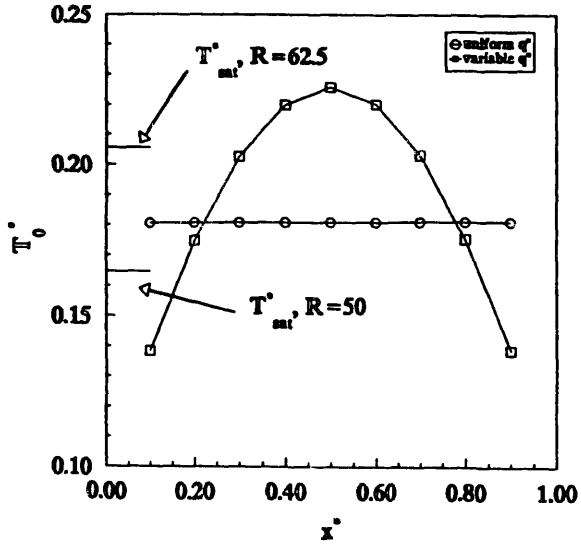

Fig. 5. Non-dimensional wall temperature for water flow and low aspect ratios, $T_s = 300$ K.

the average channel (uniform) heat flux, as discussed earlier for air flow. In each calculation, the non-dimensional mean fluid temperature $T_m^* \approx 0$ indicating a temperature ratio T_R of unity. Yet, as indicated in Fig. 5, localized boiling is calculated to occur in the central regions of the channel. Obviously in this case it is inappropriate to use the uniform heat flux results. In fact, for $50 \leq R < 62.5$, the two non-dimensional temperature profiles shown in Fig. 5 remain nearly constant but, in each case, the results from the uniform heat flux calculation entirely misrepresent the channel fluid conditions. For $R = 62.5$, the uniform heat flux results indicate that subcooled conditions exist along the entire channel but results from the more appropriate variable heat flux model predict localized boiling in the central regions of the channel. For $R = 50$, the uniform heat flux results indicate saturated conditions along the entire channel when subcooled conditions at the channel inlet and outlet are calculated with a variable heat flux. At any rate, the methods presented in this paper do not take into account two-phase fluid conditions. Consequently, erroneous results may be obtained when two-phase fluid conditions are calculated to occur.

Test reactors typically have large channel aspect ratios (Langerman, 1992). As the channel aspect ratio increases, the temperature difference between the wall and the fluid decreases. Fig. 6 shows T_0^* and T_m^* at $R = 666$ and indicates a similar trend in the wall and the fluid temperature along the channel. At the high aspect ratios, therefore, the water flow results are directly analogous to the air flow results. At lower aspect ratios, although the methods presented in the following paragraphs are valid, a check on localized subcooled boiling is recommended.

Fig. 7 shows the temperature ratio calculated with the Boussinesq and the non-Boussinesq models. Contrary to air flow, for water flow the Boussinesq model tends to overpredict the heat transfer capabilities via natural circulation, albeit to an apparently insignificant amount. This observation is consistent with the results discussed in Langerman and Bayless (1992).

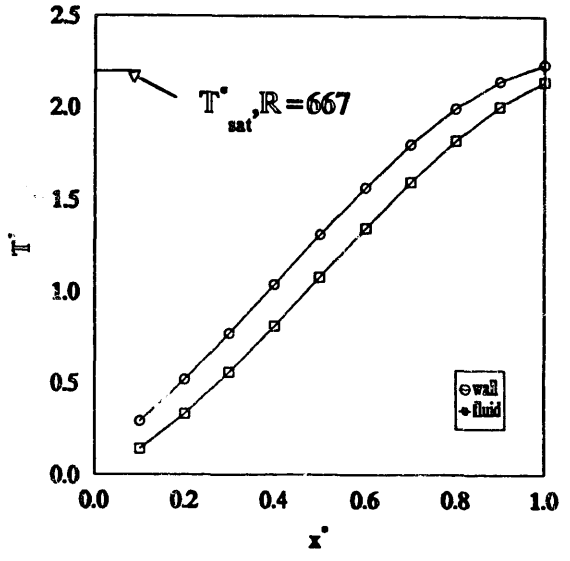

Fig. 6. Non-dimensional temperatures for water flow and large aspect ratios, $T_\infty = 300$ K.

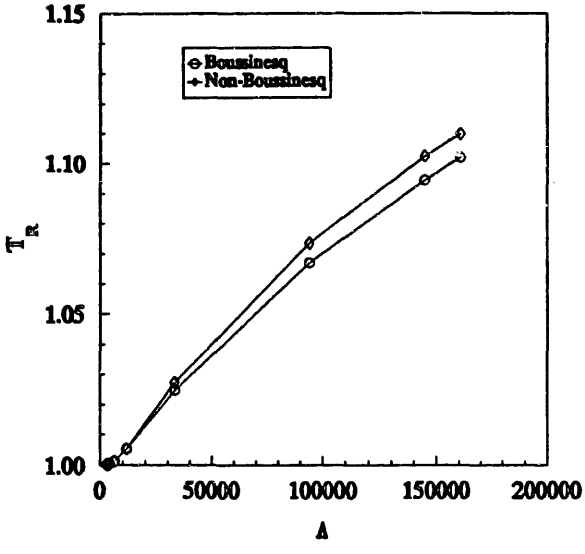

Fig. 7. Temperature ratio for water flow, $T_\infty = 300$ K.

Proceeding as before, T_{R_c} is calculated, based on a saturation temperature of 370 K, to be 1.105. Then $\Lambda_c \approx 1.5 \times 10^5$ and

$$\Phi_c = \frac{(1.5 \times 10^5)^2}{(R/S)^3} \tag{20}$$

Once again, $\Phi < \Phi_c$ does not preclude local subcooled boiling. Fig. 8 presents a plot of Φ_c *vs.* R/S. As an example, assume $R = 610$ and $L = 1.22$ m; then, Eq. (20), $\Phi_c = 180$. From Eq. (15), with $k_\infty = 0.611$ W m^{-1} K^{-1} and $T_\infty = 300$ K, $q''_{\text{avg}_c} = 2.7 \times 10^4$ W m^{-2}.

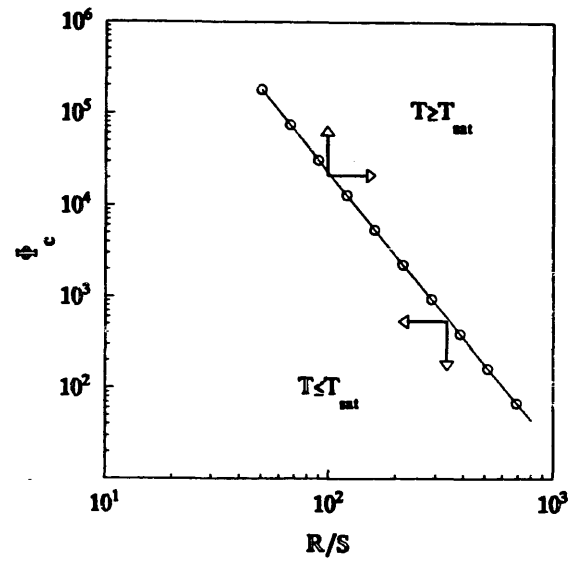

Fig. 8. Critical heat flux for water flow, $T_\infty = 300$ K.

4. Conclusions

A means for determining the critical decay heat removal rate along test reactor plate fuel, via natural circulation, has been developed, which takes into account variable fluid properties. The results indicate that the commonly applied Boussinesq model underpredicts heat transfer rates for air flow and overpredicts heat transfer rates for water flow. The non-Boussinesq results presented here are particularly useful for design and accident analysis of nuclear fuel during the storage cycle.

Acknowledgments

This work was supported, in part, by the US Department of Energy, Assistant Secretary for the Office of Nuclear Energy, under DOE Contract DE-AC07-76ID01570, and the Idaho National Engineering Laboratory Long Term Research Initiative in Computational Mechanics.

Appendix A: Nomenclature

a system parameters
b gap between plates
c_p specific heat
g gravitational constant
Gr Grashof number, $g\beta q'' b^4/\nu^2 k$
Gr_L Grashof number, $g\beta q'' L^4/\nu^2 k$
k fluid thermal conductivity
l gap half-width, $b/2$
L length of plate
$\dot{m}$ mass flow rate
M^* Eq. (17)
$\hat{p}$ pressure estimate
$\hat{p}^*$ $(\hat{p} - p_o)b^3/\rho\nu^2\,\mathrm{Gr}\,L$
p_o hydrostatic pressure
Pr Prandtl number, ν/α
q'' heat flux
R channel aspect ratio, L/b
Ra Rayleigh number, Pr Gr (b/L)
S ratio of channel length L to unit depth
T temperature
T^* $k_\infty(T - T_\infty)/q''_{avg}b$
u x direction velocity
V mean fluid velocity
V^* Pr $Vb^2/\nu L$
x, y cartesian coordinates
x^* x/L

Greek letters

α fluid thermal diffusivity
β coefficient of thermal expansion
γ_{pf} power peaking factor, q''_{max}/q''_{avg}
ϵ numerical error limit
Λ Eq. (16)
μ fluid dynamic viscosity
ν fluid kinematic viscosity
ρ fluid density
σ $(1/\mu)\,\partial\mu/\partial T$
τ wall shear stress
Φ Eq. (15)
$\tilde{\psi}$ $1 + \tilde{\sigma}(T_0 - T_m)$
$\tilde{\omega}$ $1 + 2\beta(\tilde{T} - T_m)$

Subscripts and superscripts

c critical
m mean
∞ channel inlet
0 wall

References

W. Aung, Fully developed laminar free convection between vertical plates heated asymmetrically, Int. J. Heat Mass Transfer 15 (1972) 1577–1580.

D.D. Gray and A. Giorgini, The validity of the Boussinesq approximation for liquids and gases, Int. J. Heat Mass Transfer 19 (1976) 545–551.

M.A. Langerman and P.D. Bayless, On the validity of the Boussinesq approximation for calculating decay heat removal rates via natural circulation along test reactor plate fuel, Proc. 1992 ASME Winter Annual Meeting, Anaheim, CA (ASME, 1992), HTD Vol. 209, pp. 91–100.

M.A. Langerman, A non-Boussinesq integral method for laminar free convection between vertical flat plates subject to a uniform wall heat flux, Int. J. Heat Mass Transfer 36 (1993) 3429–3435.

M. Miyamoto, H. Kajino, J. Kurima and T. Takanami, Development of turbulence characteristics in a vertical free convection boundary layer, Heat Transfer 2 (1982) 323–238.

S. Ramanathan and R. Kumar, Correlations for natural convection between heated vertical plates heated asymmetrically, J. Heat Transfer 113 (1991) 97–107.